BRINT: A BINARY ROTATION INVARIANT AND NOISE TOLERANT TEXTURE DESCRIPTOR

[1]*Li Liu*, [1]*Bing Yang,* [2]*Paul Fieguth,* [1]*Zheng Yang and* [1]*Yingmei Wei*

[1]Information System Engineering Key Lab, School of Information System and Management,
National University of Defense Technology, Changsha, China 410073
[2]Department of Systems Design Engineering, University of Waterloo, Waterloo, Canada N2L 3G1
Email:{dreamliu2010@gmail.com, yangbing@gmail.com, pfieguth@uwaterloo.ca, yz2000@263.net, weiyingmei@126.com }

ABSTRACT

Local Binary Pattern (LBP) and its variants are effective and popular descriptors for texture classification. Most LBP like descriptors have disadvantages including sensitiveness to noise and inability to capture long distance texture information. In this paper we propose a simple, efficient, yet robust multi-resolution descriptor to texture classification — Binary Rotation Invariant and Noise Tolerant (BRINT). The proposed descriptor is very fast to build, very compact while remaining robust to illumination variations, rotation changes and noise.

We develop a novel and simple strategy — averaging before binarization — to compute a local binary descriptor based on the conventional LBP approach. Points are sampled in a circular neighborhood, but keeping the number of bins in a single-scale LBP histogram constant and small by averaging over several contiguous pixels in the circle. There is no need for pre-training, no texton dictionary, and no tuning of parameters to deal with different datasets. Experiments on the Outex test suite demonstrate that the proposed approach is very robust to noise and significantly outperforms the state-of-the-art in terms of classifying noise corrupted textures.

Index Terms— Texture descriptors, rotation invariance, local binary pattern (LBP), noise robust, feature extraction, texture analysis

1. INTRODUCTION

Texture is a fundamental characteristic of the appearance of virtually all natural surfaces and is ubiquitous in natural images. Recently there has been a significant focus of attention on the design of local texture descriptors capable of achieving local invariance [1]. Among local texture descriptors, LBP [1, 2] has emerged as one of the most prominent and has attracted increasing attention in the field of image processing and computer vision due to its outstanding advantages: 1. ease of implementation, 2. no need for pre-training, 3. invariance to monotonic illumination changes, and 4. low computational complexity, making LBP a preferred choice for many applications. Although originally proposed for texture analysis, the LBP method has been successfully applied to many diverse areas of image processing: dynamic texture recognition, remote sensing, fingerprint matching, visual inspection, image retrieval, biomedical image analysis, face image analysis, motion analysis, and environment modeling (see a comprehensive bibliography of LBP methodology online).[1]

Although significant progress has been made, most LBP variants still have prominent limitations, mostly the sensitivity to noise [3], and the limiting of LBP variants to three scales, failing to capture long range texture information [3, 4]. Although some efforts have been made to include complementary filtering techniques [3,5], these *increase* the computational complexity, running counter to the goal of LBP method.

In this paper, we propose a novel, computationally simple approach, the Binary Rotation Invariant and Noise Tolerant (BRINT) descriptor, which has the following outstanding advantages: It is highly discriminative, has low computational complexity, is highly robust to noise and rotation, and allows for compactly encoding a number of scales and arbitrarily large circular neighborhoods. At the feature extraction stage there is no pre-learning process and no additional parameters to be learned.

2. BRINT: A BINARY ROTATION INVARIANT AND NOISE TOLERANT DESCRIPTOR

2.1. Motivation

Although the original LBP approach is attractive for its conceptual simplicity and efficient computation, a straightforward application of the original $\text{LBP}_{r,p}$ histogram features is limited: (1) As shown in Table 1, the original LBP operator produces rather long histograms (2^p distinct values), overwhelmingly large even for small neighborhoods, leading to poor discriminant power and large storage requirements. (2) The LBP operator captures only the very local structure of the texture, appropriate for micro-textures but not for macro-textures. Because the LBP dimensionality becomes intractable as the sampling radius increases, it is difficult to collect information from a larger area. (3) The original LBP codes are sensitive to image rotation. (4) LBP codes can be highly sensitive to noise: the slightest fluctuation above or below the value of the central pixel is treated the same way as a major contrast. The rotation invariant descriptor $\text{LBP}^{ri}_{r,p}$ has received very limited attention, having shortcomings (1,2,4) listed above and in fact providing poor results for rotation invariant texture classification [6].

The $\text{LBP}^{riu2}_{r,p}$ descriptor has avoided disadvantages (1,2), which can be seen from Table 1. However despite its clear advantages of dimensionality, gray scale and rotation invariance, and suitability for multi-resolution analysis, it suffers in terms of reliability and robustness as it only uses the uniform patterns and has minimal tolerance to noise.

The CLBP_C $*$ CLBP_S$^{riu2}_{r,p}$ $*$ CLBP_M$^{riu2}_{r,p}$, abbreviated as CLBP_CSM, has been shown to perform better than $\text{LBP}^{riu2}_{r,p}$ [7], due to the joint behavior of the three complementary LBP-like codes CLBP_C, CLBP_S and CLBP_M, although this concatenation leads to a feature vector relatively high dimensionality (Table 1). In standard CLBP_CSM applications, typically three scales are considered, with a corresponding dimensionality of 2200. The CLBC_CSM approach presented in [8], utilizes five scales to extract texture

*This work has been supported by the National Natural Science Foundation of China under contract No. 61202336 and the Doctoral Fund of Ministry of Education of China under contract No. 20124307120025.

[1]A comprehensive bibliography of LBP methodology can be found at `http://www.cse.oulu.fi/MVG/LBP_Bibliography/`.

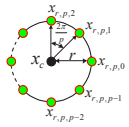

Fig. 1. Central pixel and its p circularly and evenly spaced neighbors on circle of radius r.

Table 1. Number of patterns of different descriptors. The notation CLBP_CSM is the abbreviation for CLBP_C*S$^{riu2}_{r,p}$(*M$^{riu2}_{r,p}$). The sampling schemes for scales 4 and 5 have been implemented by Zhao *et al.* [8] in their CLBC_CSM approach.

Scale	(r,p)	LBP$_{r,p}$	LBP$^{ri}_{r,p}$	LBP$^{riu2}_{r,p}$	CLBP_CSM
Scale 1	$(1,8)$	256	36	10	200
Scale 2	$(2,16)$	65536	4116	18	648
Scale 3	$(3,24)$	16777216	699252	26	1352
Scale 4	$(4,32)$	2^{32}	huge	34	2312
Scale 5	$(5,40)$	2^{40}	huge	42	3528
Scale 1-5		infeasible	infeasible	106	8040

feature, leading to an even higher dimensionality of 7530. For a multi-resolution analysis, with non-local features based on a larger number of scales, the increased dimensionality leads to challenges in storage and reliable classifier learning.

All of the discussed descriptors share one or more weaknesses of noise sensitivity, high dimensionality, and/or information insufficiency. Though all of the LBP-based approaches are computational simple at the feature extraction step, except for LBP$^{riu2}_{r,p}$ the other descriptors are all computationally expensive at the *classification* stage due to the high dimensionality of the histogram feature vector.

2.2. BRINT: Proposed Approach

Our concern with the reduced approaches of LBP^{riu2} and CLBP_CSM lies with the use of only the uniform LBP patterns, which appear to lack texture discriminability. Instead, the LBP^{ri}, although having large dimensionality, possesses meaningful texture features and strikes us as a more promising starting point.

The dimensionality of LBP$_{r,p}$ and LBP$^{ri}_{r,p}$ grow rapidly with p, so some technique of feature selection can be employed, by regrouping LBP patterns based on the observation that the occurrence probability of different LBP patterns may vary significantly. Existing strategies include two main approaches: (i) Select the most frequently occurred LBP patterns in a texture image and discard those occurring rarely [3, 9]. These methods require an extra learning process at the feature extraction stage which introduces an extra computational burden. (ii) Reclassify the nonuniform LBP patterns based on some criterion [8, 10, 11]. These approaches increase classification performance only marginally and remain noise sensitive.

2.3. BRINT_S descriptor

The construction of the local BRINT_S descriptor is illustrated in Fig. 2. Similar to the sampling scheme in the original LBP approach, we sample pixels around a central pixel x_c, however on any circle of radius r we restrict the number of points sampled to be a multiple of eight, thus $p = 8q$ for positive integer q. So the neighbors of x_c sampled on radius r are $\underline{\boldsymbol{x}}_{r,8q} = [x_{r,8q,0}, \cdots, x_{r,8q,8q-1}]^T$.

In contrast to original LBP, we transform the neighbor vector $\underline{\boldsymbol{x}}_{r,8q}$ by local averaging along an arc,

$$y_{r,q,i} = \frac{1}{q}\sum_{k=0}^{q-1} x_{r,8q,(qi+k)}, \quad i = 0, \ldots, 7, \tag{1}$$

as illustrated in Fig. 2, such that the number of neighbors in $\underline{\boldsymbol{y}}_{r,q}$ is always eight.

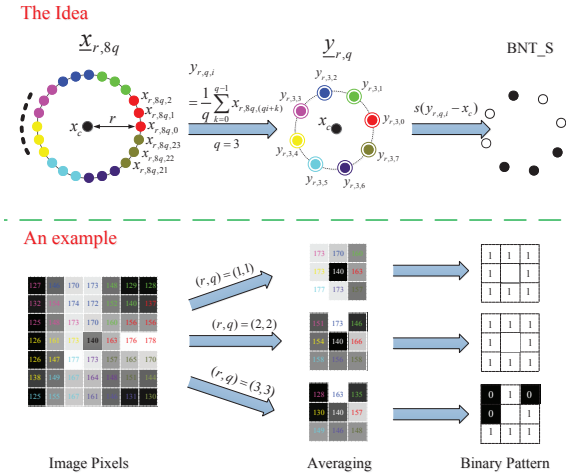

Fig. 2. Illustration of the proposed BNT_S descriptor: Rather than directly subtracting the gray value x_c of the center pixel from the precise gray value of each neighboring pixel $x_{r,8q,i}, i = 0, \ldots, 8q-1$, the proposed approach introduces an Average-Before-Quantization idea, first transforming the original neighborhood into a new one $y_{r,8q,i}, i = 0, \ldots, 7$, and then thresholding $y_{r,8q,i}, i = 0, \ldots, 7$ at the gray value of the center pixel to generate a binary pattern.

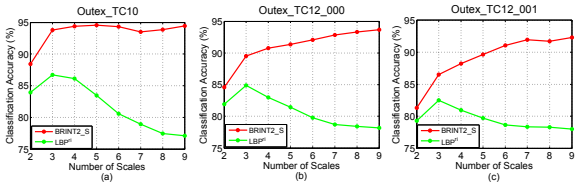

Fig. 3. Comparison of the classification accuracies of the proposed BRINT_S descriptor and the conventional LBP^{ri} descriptor, using all the three benchmark test suites from the Outex database designated by Ojala *et al.* [1]. The experimental setup is kept consistent with those in [1]. The results firmly indicate that the proposed BRINT_S descriptor significantly outperforms the conventional LBP^{ri} descriptor.

Given $\underline{\boldsymbol{y}}_{r,q} = [y_{r,q,0}, \cdots, y_{r,q,7}]^T$, we can trivially compute a binary pattern with respect to the center pixel, as in LBP:

$$\text{BNT\_S}_{r,q} = \sum_{n=0}^{7} s(y_{r,q,n} - x_c)2^n \tag{2}$$

where BNT_S represents "Binary Noise Tolerant Sign". One can easily see that for any parameter pair (r,q) there are $2^8 = 256$ BNT_S$_{r,q}$ binary patterns in total. Furthermore, the transformation from $\underline{\boldsymbol{x}}_{r,8q}$ to $\underline{\boldsymbol{y}}_{r,q}$ makes the pattern more robust to noise.

As rotation invariance is one of our stated objectives, and to avoid the limitations [3] of uniform patterns, we follow the inspiration of LBP$^{ri}_{r,q}$, grouping equal versions of binary representations under rotations, assigning code numbers to the resulting groups. Formally, then, BRINT_S$_{r,q}$ is defined as

$$\text{BRINT\_S}_{r,q} = \min\{ROR(\text{BNT\_S}_{r,q}, i) | i = 0, \cdots, 7\}, \tag{3}$$

where rotation function $ROR(\bullet, \bullet)$ is the same as in [1], reducing the number of histogram bins, for one scale, from 256 to 36. The motivation, then, for fixing the number of points in $\underline{\boldsymbol{y}}_{r,q}$ to a constant 8 was to limit the growth in histogram bins with scale.

In terms of parameter q, which controls the number of contiguous neighbors in a circle being sampled and averaged, we adopt a sampling scheme $(r,p) \in \{(1,8), (2,24), (3,24), \cdots, (r,24)\}$ as a reasonable starting point for realizing the operators, but there is no guarantee that they produce the optimal operator for a given task.

Fig. 3 validates the basic behavior of BRINT_S$_{r,q}$ as a function of the number of scales by contrasting its classification performance with that of the conventional LBP$^{ri}_{r,p}$ descriptor. The classification results show a significant jump in classification performance on the three Outex databases, outperforming the *best* results reported by Ojala *et al.* [1].

In terms of computation cost, the proposed BRINT_S descriptor does not imply an increase in complexity over the traditional LBP^{riu2}. In particular, BRINT_S always deals with local binary patterns based on 8 points, whereas for LBP^{riu2} the mapping from LBP to LBP^{riu2} requires a large lookup table having 2^p elements.

2.4. BRINT_M descriptor

Motivated by the striking classification results achieved by BRINT_S and considering the better performance of the CLBP_CSM feature over the single feature LBP^{riu2} proposed by Guo *et al.* [7], we would like to further capitalize on the CLBP_M descriptor by proposing BRINT_M.

Given a central pixel x_c and its p neighboring pixels $x_{r,p,0}, \cdots, x_{r,p,p-1}$, as before in Fig. 2, we first compute the absolute value of the local differences between the center pixel x_c and its neighbors: $\Delta_{r,8q,i} = |x_{r,8q,i} - x_c|, \quad i = 0, \cdots, 8q-1$. Following the work in [7], $\underline{\Delta}_{r,8q}$ is the magnitude component of the local difference. Similar to (2), $\underline{\Delta}_{r,8q}$ is transformed into$z_{r,q,i} = \frac{1}{q}\sum_{k=0}^{q-1}\Delta_{r,8q,(qi+k)}, \quad i = 0, \ldots, 7$. We compute a binary pattern BNT_M (Binary Noise Tolerant_Magnitude) based on $\underline{z}$ via

$$\text{BNT\_M}_{r,q} = \sum_{n=0}^{7} s(z_{r,q,n} - \mu^l_{r,q})2^n, \tag{4}$$

where μ_l is the local thresholding value. Note that the CLBP_M descriptor defined in [7] uses the global threshold, whereas in the original LBP operator the thresholding value is the center pixel value, which clearly varies from pixel to pixel. Therefore, instead of using a constant global threshold, we propose to use a locally varying one:

$$\mu^l_{r,q} = \frac{1}{8}\sum_{n=0}^{7} z_{r,q,n}. \tag{5}$$

With BNT_M defined, BRINT_M is defined as

$$\text{BRINT\_M}_{r,q} = \min\{ROR(\text{BNT\_M}_{r,q}, i)|i = 0, \ldots, 7\}. \tag{6}$$

Finally, consistent with CLBP, we also represent the center pixel in one of two bins:

$$\text{BRINT\_C}_r = s(x_c - \mu_{I,r}) \tag{7}$$

where $\mu_{I,r}$ is the mean of the whole image excluding boundary pixels:

$$\mu_{I,r} = \frac{1}{(M-2r)(N-2r)}\sum_{i=r+1}^{M-r}\sum_{j=r+1}^{N-r} x(i,j). \tag{8}$$

2.5. MultiResolution BRINT and Classification

The proposed BRINT descriptors were, so far, extracted from a single resolution with a circularly symmetric neighbor set of $8q$ pixels placed on a circle of radius r. Given that one goal of our approach is to cope with a large number of different scales, by altering r we can realize operators for different spatial resolutions, ideally representing a textured patch by concatenating binary histograms from multiple resolutions into a single histogram, clearly requiring that the histogram feature produced at each resolution be of low dimension. Since BRINT_CSM, the joint histogram of BRINT_C, BRINT_S and BRINT_M, has a very high dimensionality of $36 * 36 * 2 = 2592$, in order to reduce the number of bins needed we adopt the BRINT_CS$_{r,q}$_CM$_{r,q}$ descriptor, meaning the joint histogram BRINT_C $*$ BRINT_S$_{r,q}$ concatenated with BRINT_C $*$ BRINT_M$_{r,q}$, producing a histogram of much lower dimensionality: $36 * 2 + 36 * 2 = 144$. As a point of comparison, in the experimental results we will also evaluate BRINT_S$_{r,q}$_M$_{r,q}$, having a dimensionality of $36 + 36 = 72$.

The actual classification is performed via the simple Nearest Neighbor Classifier (NNC): The Nearest Neighbor Classifier (NNC) applied to the normalized BRINT histogram feature vectors $\underline{\boldsymbol{h}}_i$ and $\underline{\boldsymbol{h}}_j$, using the χ^2 distance metric as in [7, 12, 13].

Table 2. Summary of texture datasets used in our experiments. Scale and affine variations does not exist in the three datasets.

Texture Dataset	Image Rotation	Illumination Variation	Texture Classes	Sample Size (pixels)	Samples per Class	Training Samples per Class	Test Samples per Class	Samples in Total
Outex_TC10	√		24	128 × 128	180	20	160	4320
Outex_TC12_000	√	√	24	128 × 128	200	20	180	4800
Outex_TC12_001	√	√	24	128 × 128	200	20	180	4800

Table 3. Sampling scheme, Notations and comparisons of number of bins in the histogram feature from Single Scale (SS).

Method	Parameter	SS1	SS2	SS3	SS4	SS5	SS6	SS7	SS8	SS9
BRINT1_S	$(r,p) = (r,8q)$	$(1,8)$	$(2,16)$	$(3,24)$	$(4,32)$	$(5,40)$	$(6,48)$	$(7,56)$	$(8,64)$	$(9,72)$
(BRINT1_M)	bins	36	36	36	36	36	36	36	36	36
BRINT_S	$(r,p) = (r,8q)$	$(1,8)$	$(2,24)$	$(3,24)$	$(4,24)$	$(5,24)$	$(6,24)$	$(7,24)$	$(8,24)$	$(9,24)$
(BRINT_M)	bins	36	36	36	36	36	36	36	36	36
CLBP_S^{riu2}	(r,p)	$(1,8)$	$(2,16)$	$(3,24)$	$(4,24)$	$(5,24)$	$(6,24)$	$(7,24)$	$(8,24)$	$(9,24)$
(CLBP_M^{riu2})	bins	10	18	26	26	26	26	26	26	26
CLBP_S^{ri}	(r,p)	$(1,8)$	$(1,8)$	$(1,8)$	$(1,8)$	$(1,8)$	$(1,8)$	$(1,8)$	$(1,8)$	$(1,8)$
(CLBP_M^{ri})	bins	36	36	36	36	36	36	36	36	36

3. EXPERIMENTAL EVALUATION

3.1. Image Data and Experimental Set up

For our experimental evaluation we have used the three benchmark test suites of Ojala *et al.* [1]. There are 24 different homogeneous texture classes selected from the Outex texture database [14], with each class having only one sample of size 538×746-pixels. The 24 different texture samples are imaged under different lighting and rotations conditions. Three experimental test suites **Outex_TC10**, **Outex_TC12_000** and **Outex_TC12_001**, summarized in Table 2, were developed by Ojala *et al.* [1] as benchmark datasets for rotation and illumination invariant texture classification. For all the three test suites, the classifier is trained with 20 reference images of the "inca" illumination condition and angle 0°, totaling 480 samples.

The difference among these three test suites is in the testing set. For Outex_TC10, the remaining 3840 samples with "inca" illumination, are used for testing the classifier. For Outex_TC12_000 and Outex_TC12_001, the classifier is tested with all 4320 images from fluorescent and sunlight lighting, respectively. Clearly, Outex_TC10 is the easier of the three, since training and testing data have the same lighting.

For the experiments on all three Outex databases, we first test the classification performance of the proposed approach on the original database and then assess the robustness of the proposed method under noisy conditions, where the original texture images are corrupted by zero-mean additive Gaussian noise with different Signal-to-Noise Ratios (SNRs).

3.2. Methods in Comparison and Implementation Details

We will be performing a comparative evaluation of our proposed approach against five methods:

(1) **CLBP_CS^{ri}_CM^{ri}**: The CLBP^{ri} parallel to our proposed BRINT_CS_CM feature. (2) **CLBP_CS^{riu2}_CM^{riu2}**: The

Table 4. Comparing the classification accuracies (%) of the proposed BRINT_CS_CM descriptor with two conventional CLBP descriptors. The highest classification accuracies are highlighted in bold for each test suite.

	Single Scale									Multiple Scales							
Methods	SS1	SS2	SS3	SS4	SS5	SS6	SS7	SS8	SS9	MS2	MS3	MS4	MS5	MS6	MS7	MS8	MS9
Outex_TC10																	
BRINT_CS_CM	91.87	96.43	96.04	94.04	95.16	94.51	91.61	92.16	93.78	96.95	98.52	99.04	99.32	99.32	99.30	99.40	99.35
CLBP_CS^{ri}_CM^{ri}	91.87	95.34	89.14	84.95	80.89	78.10	73.83	70.44	67.92	96.28	95.21	93.44	91.56	90.60	89.14	88.07	87.58
CLBP_CS^{riu2}_CM^{riu2}	95.68	98.23	98.72	98.96	98.05	97.58	97.71	96.77	96.30	98.41	99.30	99.43	99.45	99.51	**99.53**	99.48	99.48
Outex_TC12_000																	
BRINT_CS_CM	86.46	93.38	94.47	91.06	92.15	89.86	89.65	89.38	90.72	94.24	96.23	97.04	97.18	97.22	97.43	97.64	**97.69**
CLBP_CS^{ri}_CM^{ri}	86.46	92.62	88.56	81.27	79.86	77.62	73.36	69.63	67.94	93.17	94.56	93.29	91.25	88.82	87.55	86.92	86.41
CLBP_CS^{riu2}_CM^{riu2}	89.81	94.31	94.88	93.98	90.56	87.85	88.26	88.29	87.71	95.63	96.81	96.67	96.23	95.95	96.00	96.00	95.97
Outex_TC12_001																	
BRINT_CS_CM	88.50	93.98	94.40	90.81	92.27	90.42	88.80	89.70	90.97	94.35	96.34	97.29	97.41	97.85	97.99	98.29	**98.56**
CLBP_CS^{ri}_CM^{ri}	88.50	93.01	87.82	81.78	79.26	76.48	73.12	69.21	68.75	93.26	93.63	92.04	90.88	89.47	88.43	87.29	86.78
CLBP_CS^{riu2}_CM^{riu2}	91.44	94.47	93.19	92.41	88.98	85.83	86.90	88.01	86.90	95.12	95.63	95.35	94.58	94.40	94.19	94.21	93.91

Table 5. Comparing the classification scores (%) achieved by the proposed approach with those achieved by recent state-of-the-art texture classification methods on the three Outex test suites. Scores are as originally reported, except those marked ($\diamond$) which are taken from the work by Guo *et al.* [7].

		Outex Database		
Classifier	Method	TC10	TC12_000	TC12_001
NNC	Ours: BRINT_CS_CM (MS9)	**99.35**	97.69	**98.56**
NNC	CLBP_CSM [7]	99.14	95.18	95.55
	CLBC_CSM [8]	98.96	95.37	94.72
	$LBP^{riu2}_{P,R}/VAR_{P,R}$ [1]	97.7	87.3	86.4
	$LBPV^{u2}_{P,R}GM^{D2-1}_{PD2}$ [12]	97.63	95.06	93.88
	$dis(S+M)^{ri}_{N,R}$ [9]		97.0	96.5
	VZ-MR8 [15]	93.59($\diamond$)	92.55($\diamond$)	92.82($\diamond$)
	VZ-Patch [16]	92.00($\diamond$)	91.41($\diamond$)	92.06($\diamond$)
SVM	DLBP+NGF [3]	99.1	93.2	90.4

$CLBP^{riu2}$ parallel to our proposed BRINT_CS_CM feature. (3) **DLBP+NGF** [3]: The fused features of the DLBP features and the normalized Gabor filter response average magnitudes (NGF). It is worth mentioning that the DLBP approach needs pretraining and the dimensionality of the DLBP feature varies with the training image. (4) **CLBP** [7]: The recommended fused descriptor CLBP_CSM is used, however only a 3-scale CLBP_CSM is implemented due to the high dimensionality limitation mentioned in Table 1. (5) **LBP** [1]: The traditional rotation invariant uniform feature proposed by Ojala *et al.* [1]. We use a 3-scale descriptor as recommended by the authors.

Each texture sample is preprocessed by normalizing to zero mean and unit standard deviation. The SNRs tested in this paper are 100, 30, 15, 10, 5 and 3, corresponding to 20db, 14.78db, 11.76db, 10db, 7db and 4.77db respectively.

3.3. Results

Fig. 4 plots the classification performance of different BRINT combination schemes as a function of number of scales. There is a trend of increasing classification performance as the number of scales increases. It is apparent that the BRINT_CS_CM feature performs the best, therefore the BRINT_CS_CM descriptor will be our proposed choice and will be further evaluated.

Table 6. BRINT performance as a function of noise, compared to CLBP and the method of Ojala *et al.* [1]. For each test Gaussian noise was added, and the highest classification accuracy highlighted in bold. The noise robustness of BRINT is quite striking.

		Classification Accuracies (%)					
Databases	Features	SNR=100	SNR=30	SNR=15	SNR=10	SNR=5	SNR=3
Outex_TC10	BRINT_CS_CM (MS9, NNC)	97.76	96.48	**95.47**	**92.97**	88.31	71.51
	CLBP_CS^{riu2}_CM^{riu2} (MS9, NNC)	**99.30**	**98.12**	94.58	86.07	51.22	28.65
	LBP^{riu2} (MS3, NNC) [1]	95.03	86.93	67.24	49.79	24.06	12.97
Outex_TC12_000	BRINT_CS_CM (MS9, NNC)	95.95	**93.59**	**91.32**	**90.49**	83.68	69.70
	CLBP_CS^{riu2}_CM^{riu2} (MS9, NNC)	**96.16**	93.54	88.73	83.52	52.22	29.35
	LBP^{riu2} (MS3, NNC) [1]	91.30	82.55	60.25	47.31	24.07	13.63
Outex_TC12_001	BRINT_CS_CM (MS9, NNC)	**96.92**	**95.14**	**93.66**	**92.29**	84.77	71.02
	CLBP_CS^{riu2}_CM^{riu2} (MS9, NNC)	95.95	93.66	88.36	81.71	53.43	26.81
	LBP^{riu2} (NNC) [1]	90.72	79.17	60.74	45.81	25.02	12.55

Table 4 compares the classification performance of the proposed BRINT_CS_CM descriptor with those of CLBP on the three Outex databases. We observe that BRINT performs significantly and consistently better than both *ri* and *riu2* forms of CLBP, both in single-scale and multiple-scale cases. The striking performance of BRINT_CS_CM clearly demonstrates that the concatenated marginal distributions of the proposed basic BRINT_C, BRINT_S and BRINT_M codes and the novel "averaging before binarization" scheme turns out to be a very powerful representation of image texture. The use of multiple scales offers significant improvements over single-scale analysis, consistent with earlier results in Fig. 4, showing that the approach is making effective use of interactions between the center pixel and more distant pixels. To the best of our knowledge, the proposed approach produced classification scores which we believe to be the best reported for Outex_TC12_000 and Outex_TC12_001. Keeping in mind the variations in illumination and rotation present in the Outex databases, the results in Table 4 firmly demonstrate the illumination and rotation invariance property of the proposed BRINT_CS_CM approach.

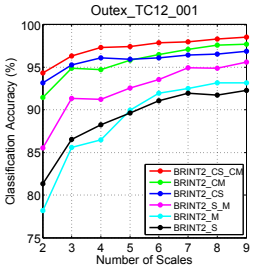

Fig. 4. Classification rates as a function of number of scales, with the same experimental setup as in Fig. 3, using a NNC classifier. Of the combinations tried, BRINT_CS_CM performs the best.

Table 5 compares the best classification scores achieved by the proposed BRINT_CS_CM method using nine scales (MS9) in comparison with state-of-the-art texture classification methods on all three Outex test suites. Despite not being customized to the separate test suites, our multi-scale BRINT descriptor produces what we believe to be the best reported results on all three suites. We would also point out that except for the proposed BRINT, CLBP_CSM [7] and CLBC_CSM [8] approaches, the remaining descriptors listed in Table 5 require an extra learning process to obtain the texton dictionary, requiring additional parameters or computational burden.

The preceding discussion allows us to assert that the proposed multi-scale BRINT approach outperforms the conventional multi-scale CLBP approach on the Outex test suites. We now wish to examine the robustness of our method against noise to test applicability to real-world applications, thus the original texture images have been subject to added Gaussian noise.

Table 6 quite clearly shows the noise-robustness offered by the BRINT approach: similar classification rates are seen in the near-absence of noise (SNR=100), however the degree to which BRINT outperforms LBP and CLBP becomes more and more striking as SNR is reduced, with classification rates more than 40% higher over CLBP and LBP at very low SNR.

4. CONCLUSIONS

In this paper we have presented BRINT, a theoretically and computationally simple, noise tolerant approach to texture classification. The method is efficient, robust to additive noise, illumination and rotation invariant, avoiding the drawbacks associated with uniform patterns, and capable of encoding a large number of scales. The proposed approach produces consistently good classification results on all of the datasets, most significantly outperforming the state-of-the-art in cases of high noise.

5. REFERENCES

[1] T. Ojala, M. Pietikäinen, and T. Maenpää, "Multiresolution gray-scale and rotation invariant texture classification with local binary patterns," *IEEE Trans. Pattern Anal. Mach. Intell.*, vol. 24, no. 7, pp. 971–987, Jul 2002.

[2] T. Ojala, M. Pietikäinen, and D. Harwood, "A comparative study of texture measures with classification based on feature distributions," *Pattern Recognit.*, vol. 29, no. 1, pp. 51–59, 1996.

[3] S. Liao, M.W.K. Law, and A.C.S. Chung, "Dominant local binary patterns for texture classification," *IEEE Trans. Image Process.*, vol. 18, pp. 1107–1118, 2009.

[4] T. Mäenpää and M. Pietikäinen, "Multi-scale binary patterns for texture analysis," in *SCIA*. IEEE, 2003, pp. 885–892.

[5] T. Ahonen, J. Matas, C. He, and M. Pietikäinen, "Rotation invariant image description with local binary pattern histogram fourier features," in *Proc. Scand. Conf. Image Anal.* IEEE, 2009, pp. 61–70.

[6] M. Pietikäinen, T. Ojala, and Z. Xu, "Rotation-invariant texture classification using feature distributions," *Pattern Recognition*, vol. 33, pp. 43–52, 2000.

[7] Z. Guo, L. Zhang, and D. Zhang, "A completed modeling of local binary pattern operator for texture classification," *IEEE Trans. Image Process.*, vol. 9, pp. 1657–1663, 2010.

[8] Y. Zhao, D. Huang, and W. Jia, "Completed local binary count for rotation invariant texture classification," *IEEE Trans. Image Process.*, vol. 21, pp. 4492–4497, 2012.

[9] Y. Guo, G. Zhao, and M. Pietikäinen, "Discriminative features for texture description," *Pattern Recognit.*, vol. 45, pp. 3834–3843, 2012.

[10] L. Liu, P. Fieguth, G. Kuang, and D. Clausi, "Sorted random projections for robust rotation invariant texture classification," *Pattern Recognition*, vol. 45, pp. 2405–2418, 2012.

[11] L. Nanni, S. Brahnam, and A. Lumini, "A simple method for improving local binary patterns by considering nonuniform patterns," *Pattern Recognition*, vol. 45, pp. 3844–3852, 2012.

[12] Z. Guo, L. Zhang, and D. Zhang, "Rotation invariant texture classification using lbp variance (lbpv) with global matching," *Pattern Recognit.*, vol. 43, pp. 706–719, 2010.

[13] Li Liu and P. Fieguth, "Texture classification from random features," *IEEE Transactions on Pattern Analysis and Machine Intelligence*, vol. 34, no. 3, pp. 574 –586, March 2012.

[14] T. Ojala, T. Mäenpää, M. Pietikänen, J. Kyllönen J. Viertola, and S. Huovinen, "Outex–new framework for empirical evaluation of texture analysis algorithms," in *Proc. 16th Int. Conf. Pattern Recognit.*, 2002, pp. 701–706.

[15] M. Varma and A. Zisserman, "A statistical approach to texture classification from single images," *Int. J. Comput. Vision*, vol. 62, no. 1-2, pp. 61–81, 2005.

[16] M. Varma and A. Zisserman, "A statistical approach to material classification using image patches," *IEEE Trans. Pattern Anal. Mach. Intell.*, vol. 31, no. 11, pp. 2032–2047, 2009.